Original Research

DIGITAL HEALTH

DIGITAL HEALTH
Volume 9: 1–19

DOI: 10.1177/20552076231180054
journals.sagepub.com/home/dhj

Sage

MonDiaL-CAD: Monkeypox diagnosis via selected hybrid CNNs unified with feature selection and ensemble learning

Omneya Attallah

Abstract

Objective: Recently, monkeypox virus is slowly evolving and there are fears it will spread as COVID-19. Computer-aided diagnosis (CAD) based on deep learning approaches especially convolutional neural network (CNN) can assist in the rapid determination of reported incidents. The current CADs were mostly based on an individual CNN. Few CADs employed multiple CNNs but did not investigate which combination of CNNs has a greater impact on the performance. Furthermore, they relied on only spatial information of deep features to train their models. This study aims to construct a CAD tool named "Monkey-CAD" that can address the previous limitations and automatically diagnose monkeypox rapidly and accurately.

Methods: Monkey-CAD extracts features from eight CNNs and then examines the best possible combination of deep features that influence classification. It employs discrete wavelet transform (DWT) to merge features which diminishes fused features' size and provides a time-frequency demonstration. These deep features' sizes are then further reduced via an entropy-based feature selection approach. These reduced fused features are finally used to deliver a better representation of the input features and feed three ensemble classifiers.

Results: Two freely accessible datasets called Monkeypox skin image (MSID) and Monkeypox skin lesion (MSLD) are employed in this study. Monkey-CAD could discriminate among cases with and without Monkeypox achieving an accuracy of 97.1% for MSID and 98.7% for MSLD datasets respectively.

Conclusions: Such promising results demonstrate that the Monkey-CAD can be employed to assist health practitioners. They also verify that fusing deep features from selected CNNs can boost performance.

Keywords

Monkeypox disease, computer-aided diagnosis, deep learning, ensemble classification, feature selection

Submission date: 9 March 2023; Acceptance date: 18 May 2023

Introduction

There have been various viral disease epidemics over the last 20 years such as COVID-19 initiated in 2019. The entire globe has only recently begun recovering from the novel coronavirus pandemic, but the appearance of monkeypox in 2022 indicates the emergence of a new worldwide virus.[1,2] The Congo revealed its first instance of a human infection caused by a monkeypox viral illness in 1970. Ever since then, monkeypox has been regarded among the most threatening orthopoxviral for public health. Monkeypox used to be most common virus in West African countries. Nevertheless, it has recently been observed in urban regions out beyond Africa.[3] Because of monkeypox's quick propagation in 19 countries beyond the outbreak zones,[4] the recent multi-region pandemic of the monkeypox disease poses a serious worldwide health

Department of Electronics and Communications Engineering, College of Engineering and Technology, Arab Academy for Science, Technology and Maritime Transport, Alexandria, Egypt

Corresponding author:
Omneya Attallah, Department of Electronics and Communications Engineering, College of Engineering and Technology, Arab Academy for Science, Technology and Maritime Transport, Alexandria 1029, Egypt.
Email: o.attallah@aast.edu

concern.[5] The globe could not afford a further disease outbreak, while the effects of the previous one are still being felt.

Monkeypox can be diagnosed primarily using the polymerase chain reaction (PCR) technique or a skin lesion check using electron microscopy. PCR is currently the most common technique of virus verification, and it has lately been employed for COVID-19 diagnosis.[6–9] However, PCR has several drawbacks such as being expensive and time-consuming, and there are insufficient kits in rural regions.[10,11] Besides, the tiny variations in skin irritation among various maladies (e.g. chickenpox, measles, and cowpox) combined with the rareness of monkeypox disease made early recognition extremely difficult using images produced with electron microscopy.[12] Early diagnosis of monkeypox is critical for reducing the propagation of this virus around the globe, isolating infected cases, and following adequate treatment of infected cases. However, the early detection procedure is complex as discussed earlier. Therefore, automated approaches are essential to facilitate the primary detection and diagnosis of monkeypox disease.

During the COVID-19 global epidemic, scientists and health providers learned the importance of precise and timely disease detection in order to prevent subsequent outbreaks from causing indescribable morbidity. As was observed throughout the prior disease epidemic, the techniques of artificial intelligence (AI), along with their exceptional developments and use in the healthcare system, have transformed into valuable tools for illness detection and computer-aided diagnosis (CAD) systems to assist in disease diagnosis and precise clinical identifications of several diseases such as breast cancer,[13–15] brain tumors and disorders,[16–19] stomach illness,[20] and eye diseases.[21,22] Besides, AI has shown great success in other application domains such as renewable energy,[23,24] industry,[25] and agriculture.[26] Consequently, analogous applications for detecting monkeypox cases can be established.[27,28] Images of infected individual skin can be collected and used to identify this illness with adopted machine-learning approaches including deep learning.

In the present study, a CAD framework named MonDiaL-CAD classifies patients' skin images into two groups (i.e. monkeypox and negative including chicken pox, healthy, and measles). The framework's main goal is to disclose an accurate decision using a blend of pre-trained convolutional neural network (CNN) deep learning models and machine learning classification methods. CNN is deemed as the most potent deep learning algorithm proficient in solving the issue that this research seeks to address image classification;[29] thus it is employed in this study. The proposed CAD utilizes eight CNNs to extract deep features rather than employing a single model like most of the previous studies. Furthermore, instead of directly combining features of these CNNs as in the case of existing CAD systems, MonDiaL-CAD searches for the best mixture of deep feature sets acquired from eight CNNs using a forward search strategy. In addition, current CAD models depend on learning the classification models with only spatial data acquired from skin images; however, MonDiaL-CAD uses discrete wavelet transform (DWT) to fuse these feature sets and reduce their dimensions and obtain time-frequency representations of features which usually enhance detection accuracy. Additionally, in contrast with present CADs, MonDiaL-CAD employs a feature selection technique to further lessen the attribute length, thus decreasing classification complexity. Finally, it employs ensemble approaches to enhance classification results.

The novelty and contribution of the present CAD are shown below:

- Obtaining multiple deep features from several CNNs of different structures instead of relying on one CNN opposing the case in existing CADs.
- Investigating the best combination of deep feature sets using a forward search strategy instead of using all deep feature sets obtained from the multiple CNNs, thus lowering the features' space size and number of CNNs employed to construct the proposed CAD.
- Combining every possible combination of deep feature sets via DWT is helpful as it reveals the time-frequency interpretations of deep attributes and performs a reduction step.
- Training the classification models based on spatial-time-frequency features rather than utilizing spatial attributes only dislikes what is done in current studies.
- Presenting a feature selection approach to select significant deep features and reduce feature dimension which correspondingly lower classification computational cost.
- Employing ensemble classification methods such as Bagging, Random Subspace, and Rotation Forest to boost performance.

The steps of the study design are as follows. First of all, the research problem/question that the study will explore is defined. This research problem/question involves detecting monkeypox disease from skin lesion images and distinguishing it from non-monkeypox cases including comparable diseases such as chickenpox and measles using a selected hybrid set of deep learning models. Next, in order to address this research problem, an experimental research design is conducted. A secondary data collection procedure is identified where data is gathered through extensive, manual investigations of websites, news portals, and publicly available case reports. Afterward, data is analyzed in a quantitative approach using several deep learning models constructed using MATLAB R2020a. Eight CNN deep learning models are created, and deep features are extracted from these CNNs. The literature has shown that fusing deep features can boost

performance,[30–32] however selecting which combination of CNN deep features is not well studied in previous related works for monkeypox diagnosis. Therefore, in this study, a forward search strategy is then employed to select the best set of combined deep features. Note that fusion is done using the DWT which could convey the time-frequency illustration of the input which frequently boosts performance.[33] Then, the selected fused deep feature size is reduced using a feature selection approach based on entropy.

Literature review

In 1970, the very first human incident of monkeypox was reported. Thereby, research on human monkeypox in the literature extends back to the 1970s.[34] The study of human monkeypox has recently upped due to the rapid spread of monkeypox infection globally. Lately, some scholars[35] stated in their study results that further research on this subject is required. Even though human monkeypox illness has been around for a long time, CAD-based studies for primary diagnosis have only recently started. There is currently very little research on it. The insufficiency of CADs created for image-based analysis of monkeypox has been caused by the absence of a publicly released dataset for purposes of training and testing because the virus has only recently been broadly initiated in several countries.[36] All of these CADs employed CNNs due to their great capacity in analyzing medical images and extracting significant patterns of several diseases.[37] Transfer learning (TL) has been adopted in these studies to perform classification. TL is a new branch of AI extensively used in a variety of medical image analysis and diagnosis disciplines. It allows a model that has been learned with a huge dataset on one task (known as a pre-trained model) to be re-purposed on a smaller dataset for another comparable task.[38] This process consequently accelerates training and boosts the efficiency of deep learning models.[39]

The initial research that investigated monkeypox diagnosis is the study by Ahsan et al.[40] where the authors collected images of patients infected by monkeypox from various online accessible portals. Furthermore, the same authors in[41] developed a modified version of the VGG CNN model using TL. Later, the study[6] investigated the utilization of 13 pre-trained CNNs after adding global custom layers. The authors then combined their predictions using majority voting. Furthermore, the study[42] utilized six CNNs separately to distinguish images with monkeypox from images with other diseases and normal cases using another new dataset collected from online sources called Monkeypox Skin Lesion Dataset (MSLD).[43] These CNNs include ResNet-18, MobileNet, NasNetMobile, GoogLeNet, EfficientB0, and ShuffleNet, where the highest performance was achieved with MobileNet. The same dataset (MSLD) was used in[44] to train the ResNet-18 CNN model with TL. Similarly, the studies[45,46] employed the MSLD dataset to identify monkeypox using a new version of GoogLeNet called MiniGoogLeNet. In contrast, the study[30] utilized the MSLD dataset to train three CNNs involving Inception, Xception, and DenseNet-169. The authors then combined predictions of these three CNNs via the Beta function-based normalization method. On the other hand, the research article[31] fused features of DenseNet and EfficientB0 fed with the MSLD dataset.

A further dataset was introduced called Monkeypox Skin Image Dataset (MSID)[47] and was utilized in a number of studies. For example, the study[3] proposed a new approach for fine-tuning customized CNN layers for identifying monkeypox disease from photos utilizing AI-Biruni Earth radius (BER) optimization-based stochastic fractal search (BERSFS). Likewise, the research article[36] employed the BER optimization approach along with the sine cosine (SC) procedure and the particle swarm (PS) optimization process to select features extracted from four CNNs separately using TL and optimized parameters of a multilayer perceptron (MLP) classifier. These CNNs involve ResNet-50, AlexNet, GoogLeNet, and VGG-19 where GoogLeNet achieved the highest performance. On the other hand, the study[12] employed several CNNs independently including VGG-19, VGG-16, Xception, and MobileNet, The hyperparameters of these CNNs were optimized by means of a Harris Hawks Optimizer (HHO) algorithm. Features were then extracted from such CNNs and fed to seven classifiers, and then the best predictions of these classifiers are fused with majority voting. The VGG-19 predictions fused with support vector machine (SVM) and random forest (RF) results obtained the peak performance, whereas the article[48] used three CNNs including VGG-16, VGG-19, and MobileNet on the MSID dataset where the highest performance is reached with MobileNet. The authors of[49] constructed a modified version of DenseNet-201 and trained it using the original images of the MSID dataset to diagnose monkeypox and differentiate it from other comparable diseases. The study[27] employed several CNN architectures independently to differentiate between monkeypox and non-monkeypox cases. The authors employed both the MSID and MSLD datasets to validate their models.

Other authors collected their datasets through a web search of available skin images of monkeypox, chickenpox, and other diseases. For instance, the research article[50] gathers data on monkeypox and chickenpox through a web search. The authors used the acquired data to train and test a customized CNN model to recognize monkeypox. Similarly, the study[51] explored websites, online portals, newspapers, and freely distributed samples to search for monkeypox and normal images. The authors then presented Generalization and Regularization (GR)-based TL with ten CNNs to distinguish between monkeypox and normal images. In contrast, the study[52] acquired data on monkeypox as a positive class in addition to Lyme, pityriasis rosea rash, drug rash, and ringworm infections as a negative class from online sources and

combined it with the MSLD dataset. The authors then utilized this dataset to construct five CNNs with different optimization approaches to distinguish monkeypox from other comparable diseases, whereas the authors of[28] utilized for different CNNs and independently and combined to identify monkeypox and find out that the highest performance is attained with GoogLeNet and ResNet combined.

Table 1 summarizes the literature. It can be observed from Table 1 that most of the studies employed individual CNN models to either perform classification or extract features; nonetheless combining features or predictions from multiple CNNs can boost performance.[53–55] In addition, the few studies[6,12,30,31] which employed CNN ensembles did not search for the best combination of deep feature sets extracted from district CNNs, whereas searching for the best combination can improve performance with a less number of CNNs and deep features. Furthermore, all of these studies relied on spatial features only to achieve classification, while time-frequency descriptors along with spatial information representations can enhance classification results.[33,56] Additionally, most of the existing CADs did not employ a feature selection (FS) approach to reduce the dimensionality of feature space and select the best significant features, to overcome these limitations existing in current CADs. This study introduces a novel CAD that employs several CNNs of distinct architectures. It searches for the best combination of deep feature sets obtained from these CNNs using a forward search strategy instead of using all CNNs' deep features. The introduced CAD while investigating deep feature sets fuses each possible combination of deep feature sets employing DWT that is capable of presenting the time-frequency demonstration within deep attributes. Thus, the classification models of the proposed CAD are trained with spatial-time-frequency descriptors not only spatial information. The CAD accomplishes a feature selection approach to select significant features and reduce feature dimensionality, thus lowering the complexity of the classification process. Finally, the proposed CAD utilizes ensemble classification models like Bagging, Random Subspace, and Rotation Forest to boost performance.

Materials and methods

Monkeypox datasets

Monkeypox Skin Image Dataset. The experiments that will be carried out in this paper will be constructed on two publicly available datasets. The initial dataset is called MSID.[47,49] Recently, with the initiation of monkeypox occurrence, healthcare experts across the globe have expressed concerns about diagnosing such a disease. To reach this aim, a new skin image-based set of data devoted to the diagnosis of monkeypox illness has been created. This collection included 293 photos of healthy subjects, 279 of monkeypox, 107 pictures of chickenpox cases, and 91 photos of cases of measles. All images were gathered using Internet-based sources. In this study, in order to perform binary classification, all chickenpox and measles images are combined with 100 normal images forming the negative class, while the entire images of monkeypox form the monkeypox class. Examples of the images located in each class of the MSID dataset are displayed in Figure 1.

Monkeypox Skin Lesion Dataset. The other dataset utilized to conduct the experiments of this article is called Monkeypox Skin Lesion Dataset.[43] The dataset contains 228 photographs, 102 of which are from the monkeypox category and 126 from the non-monkeypox category. Instances of photos available in each category are displayed in Figure 2. The monkeypox skin lesion datasets were basically assembled by intensive manual explorations of openly accessible case reports, news portals, and websites. Automated web scrapers were not used. With the aid of Google's Reverse Image Search, every single one of the skin lesion pictures found online was checked, and the outcomes were combined with data from other sources. Inclusion–exclusion criteria are as follows: The poor-quality, weak-resolution, and negligible-of-focus photographs were eliminated through a two-stage screening process, leaving only the distinctive images that meet the standards for quality.

Proposed MonDiaL-CAD for monkeypox diagnosis

The proposed MonDiaL-CAD consists of six stages that are summarized as follows: photo preprocessing and augmentation, pre-trained CNN building, deep feature extraction and ranking, deep feature set fusion and selection, deep feature selection, and finally diagnosis with ensemble learning. The various stages of MonDiaL-CAD are shown in Figure 3. The first block of Figure 3 represents the photo preprocessing stage, where primarily images of both datasets are preprocessed including resizing and augmentation. Subsequently, in the pre-trained CNN building stage which is the second block of Figure 3, numerous pre-trained CNNs are constructed and trained with these photos. After that, the third block of Figure 3 shows the deep feature extraction and ranking stage. In this stage, deep features are acquired from these CNNs and then utilized individually to feed an SVM model. The diagnostic accuracy achieved by the SVM classifier is utilized to rank these deep feature sets generated. Next, in the fourth block of Figure 3 which resembles the deep feature set fusion and selection stage, the space of deep feature sets is examined using a forward strategy to choose the best possible combination of deep feature sets which boost performance, where feature sets in this stage are fused using DWT. Afterward, in the fifth block of Figure 3 revealing the deep feature selection stage, a feature selection method is employed to decrease the aspect of the selected combined deep feature sets. Finally, the last block of Figure 3 demonstrates the diagnosis with an ensemble learning stage in

Table 1. Summary of the literature.

Study	Dataset	#Images after augmentation	methods	Classification	Accuracy
[41]	Monkeypox2022 # images = 164	1915	Modified VGG-16	Binary (monkeypox vs. chickenpox) (monkeypox vs. others)	83.0% 78.0%
[6]	Monkeypox2022 # images = 164	1755	VGG-16 + ResNet-50 + VGG-19 + ResNet-101 + Inception + MobileNet + InceptionResNet + XceptionEfficientB0 + Efficient-B1 + Efficient-B2 + DenseNet-121 + DenseNet-169 + majority voting	Multiclass (monkeypox vs. chickenpox vs. measles vs. normal)	87.13%
[57]	Monkeypox2022	41,503	MobileNet	Multiclass (monkeypox vs. chickenpox vs. measles vs. cowpox vs. smallpox vs. normal)	99.25%
[42]	Monkeypox Skin Lesion Dataset (MSLD)[43] #images = 228	3192	MobileNet	Binary (monkeypox vs. others)	91.11%
[44]	MSLD	3192	ResNet-18	Binary (monkeypox vs. others)	99.81%
[45]	MSLD	2067	MiniGoogLeNet	Binary (monkeypox vs. others)	97.08%
[30]	MSLD	Unspecified	Inception + Xception + DenseNet-169 + Beta function-based normalization method	Binary (monkeypox vs. others)	93.39%
[31]	MSLD	Unspecified	EfficientB0 + DenseNet	Binary (monkeypox vs. others)	94.57%
[58]	MSLD	3192	ResNet-50	Binary (monkeypox vs. others)	94.0%
[3]	MSID #images = 770	N/A	customized CNN + BERSFS	Multiclass (monkeypox vs. chickenpox vs. measles vs. normal)	98.83%
[36]	MSID	Unspecified	GoogLeNet + BER + SC + PS + MLP	Binary (monkeypox vs. others)	93.8%
[12]	MSID	Unspecified	HHO + VGG-19 + RF + SVM + Majority voting	Binary (monkeypox vs. others)	97.67%
[48]	MSID	N/A	MobileNet	Multiclass (monkeypox vs.	91.38%

(continued)

Table 1. Continued.

Study	Dataset	#Images after augmentation	methods	Classification	Accuracy
				chickenpox vs. measles vs. normal)	
[49]	MSID	N/A	DenseNet-201	Multiclass (monkeypox vs. normal vs. chickenpox vs. measles)	91.91%
[50]	MSLD + chickenpox images online #images = 342	20,100	Customized CNN	Binary (monkeypox vs. chickenpox)	99.6%
[51]	Private #images = 1830 Monkeypox2022	unspecified	GL + Xception GL + ResNet-101	Binary (monkeypox vs. normal) Multiclass (monkeypox vs. normal vs. chickenpox vs. measles)	94% 99%
[52]	Customized dataset + MSLD	2056	MobileNet	Binary (monkeypox vs. others)	96.8%
[27]	MSID MSLD	477 328	EfficientNet-B4, ResNet-50, MobileNet, Inception-V2	Binary (monkeypox vs. others)	96.5% 93%
[28]	Customized dataset	150	ResNet18 + GoogLeNet	Binary (monkeypox vs. others)	91.57%

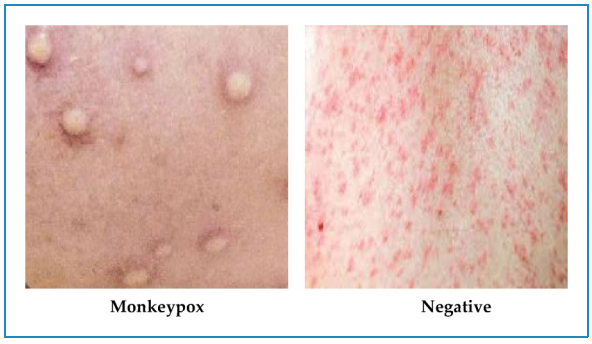

Figure 1. Examples of the images located in each class of the MSID dataset.

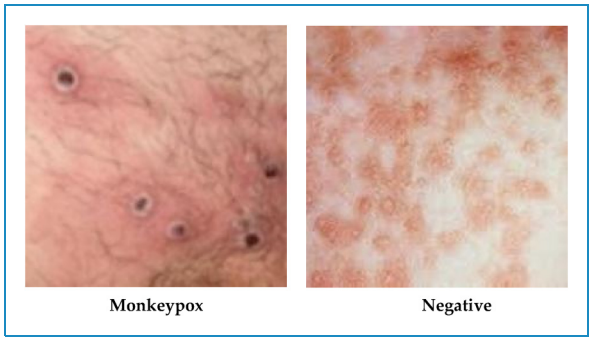

Figure 2. Instances of the images located in each class of MSID dataset.

which ensemble classifiers are built to perform the diagnosis.

Photos preprocessing and augmentation. Photographs of the two datasets are initially resized to be applicable to feed each CNN's input layer dimension. Their dimensions are altered to $224 \times 224 \times 3$ for ResNet-18, ResNet-50, ResNet-101, Shuffle, and MobileNet. For Inception and Xception images, aspects are changed to $229 \times 229 \times 3$, while for DarkNet-53, they are changed to $256 \times 256 \times 3$. After that, these images are split into 70%–30% for training and testing. To improve the learning capability of CNNs, an augmentation technique is vital. Augmentation decreases the possibility of overfitting by generating replicas of the training images, thus increasing the number of photos used to train CNNs which leads to improving performance and preventing overfitting.[59,60] The approaches for augmentation utilized in this work are transformation,

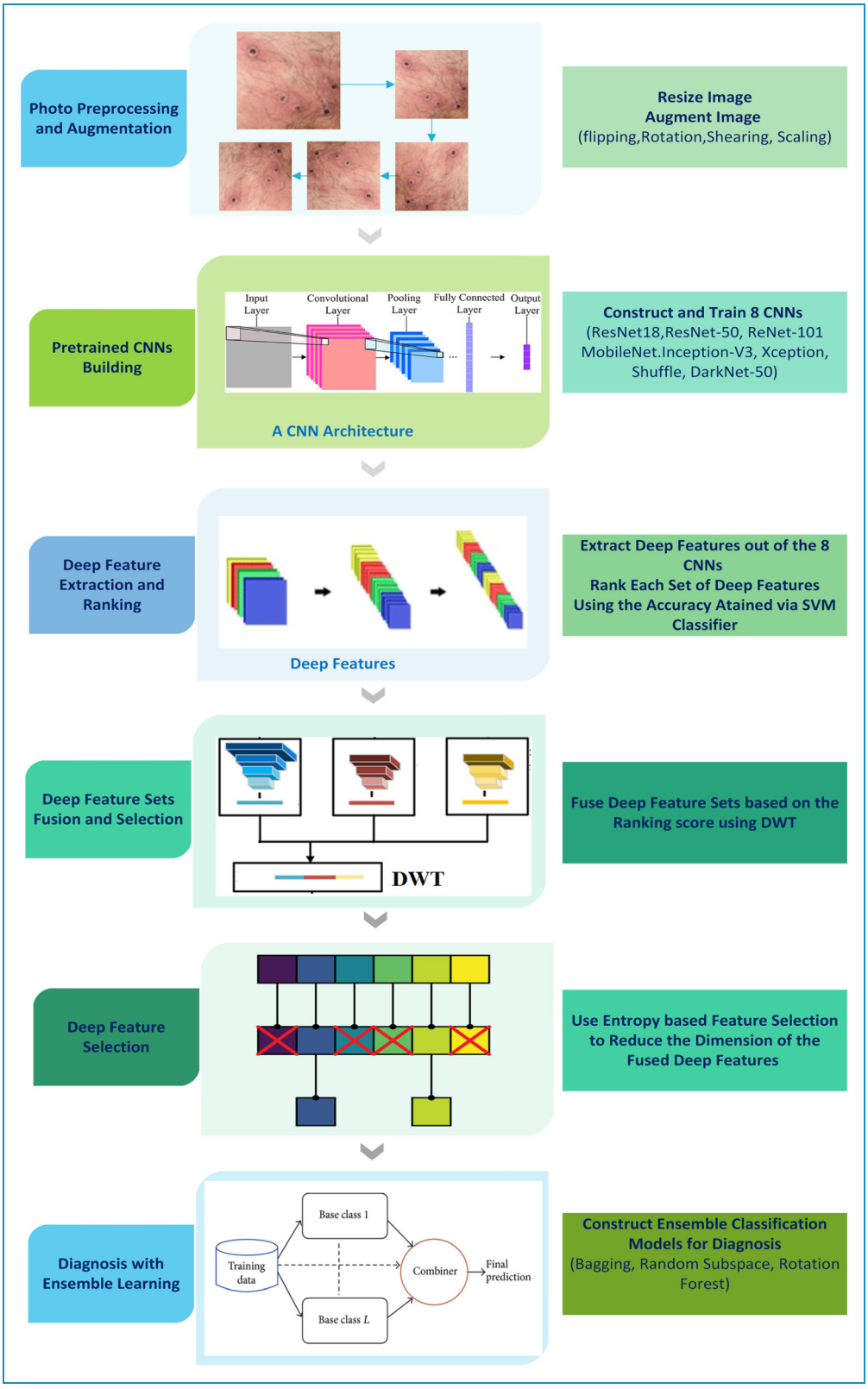

Figure 3. Various stages of the proposed MonDiaL-CAD.

Table 2. Deep feature extraction layer title and deep features length.

CNN Model	Deep Feature Sets Extraction Layer Title	Deep Features Length
Shuffle	"node 200"	544
ResNet-18	"pool5"	512
ResNet-50	"avg_pool"	2048
ResNet-101	"pool5"	2048
MobileNet	"global_average_pooling2d_1"	1280
Inception-V3	"avg_pool"	2048
Xception	"avg_pool"	2048
DarkNet-53	"avg_1"	1024

scaling, vertical and horizontal flipping, and vertical and horizontal shearing.

Pre-trained CNN building. In this work, eight pre-trained CNNs that were priorly learned on ImageNet are implemented using TL. These CNNs involve ResNet-18, Shuffle, MobileNet, ResNet-50, Inception, Xception, ResNet-101, and DarkNet-53. The reasons for choosing such CNNs are that most of them have been used in the literature. Also, each one of them has a unique architecture and advantage, and merging these advantages could probably improve performance. The number of fully connected layers of every CNN is modified to be equal to 2 corresponding to the amount of labels (monkeypox versus negative) used in the experiments performed in this work. Following that, a few hyper-parameters are regulated, which is debated afterward in the experiment installation section. After that, such CNNs are re-trained using the images of the MSID and MSLD datasets.

Deep feature set extraction and ranking. Deep attributes are obtained via TL out of the latest pooling layer just after the re-training process has been finished. The CNN structure has various layers; earlier ones discover the underlying elements within a photograph, whereas the subsequent layers locate comprehensive aspects of the image. Hence, the last pooling layer is chosen to retrieve deep feature sets. A further justification is that because the latter layers acquire attributes of lesser dimensional space, and because pooling layers lower the dimension of features, deep feature sets are obtained from the last pooling layer. The length of each deep feature set and the title of the layer upon which features are extracted are discussed in Table 2. These features are then employed separately to train an SVM classifier. The classification accuracy attained using this classifier is then used to rank these deep feature sets generated.

Deep feature set fusion and selection. According to the ranking score obtained in the previous stage, deep features are investigated in a forward search strategy to find out the best possible merged deep feature sets that boost performance. The forward strategy initiates with the deep feature set having the highest-ranking record and then adds iteratively the subsequent deep feature set. Only if the classification accuracy is improved, then this deep feature set remains; otherwise it is eliminated. Note that, throughout the deep feature sets, deep feature sets are fused using DWT. DWT is a commonly used signal-processing method that interprets input data simultaneously in the domains of time and frequency. It uses multiple filters to separate input data into the low-pass and high-pass aspects.[61] The low-pass filtered section contains information about gradually evolving input attributes, while the high-pass filtered section contains information about abrupt shifts in feature representation.[62] Multilevel DWT is achieved by allowing the low-pass filtered section to reenter a number of low- and high-pass filters to further analyze input data. DWT demonstrates as mentioned before the time-frequency representations of input data. It is also used to compress input data. Therefore, DWT is employed in this study to fuse deep feature sets which after analyzing the combined deep feature sets provide spatial-time-frequency demonstrations that could improve the diagnostic process. Note that the dimensions of the deep feature sets after fusion are reduced using the DWT process. In this work, two levels of DWT are conducted with the "Haar" mother wavelet.

Deep feature selection. Feature selection is a vital task in determining the highly critical attributes among all features to pinpoint their dimension, which improves detection capability and precludes overfitting.[63–65] Thus, in this work, a feature selection approach based on entropy is employed to reduce the feature space aspect and select the considerable ones. Entropy is an important metric for assessing the uncertainty of random variables. When a random variable has an equal chance of taking all possible values, the entropy is maximized. Once the random variable gets one value with a likelihood equal to 1, it gets the minimum entropy.[66] The larger the entropy of an attribute, the less information it contains (the more costly the process of entropy decreases) because its appointed weight is lower. To begin calculating the entropy of a feature, the

uncertainty function c is described as[67]:

$$c = \log\left(\frac{1}{p}\right) = -\log(p) \quad (1)$$

where p denotes the related probability. So, the quantification of information entropy $E(C)$ could be noticed by determining the probability of the uncertainty function:

$$E(C) = \sum_{c \in C} c.p = -\sum plog(p) \quad (2)$$

where C denotes the collection of all possible events.

Diagnosis with ensemble learning. To rank deep feature sets and perform the deep feature selection procedure, a linear SVM classifier is used. However, in this final stage of the diagnosis procedure, the MonDiaL-CAD is accomplished using ensemble classification. The concept behind ensemble classification is to train a collection of classifiers, known as an ensemble of classifiers, and afterward merge their outputs for the recognition of unforeseen cases via some type of voting. The ensemble of classifiers is usually expected to have a higher level of prediction performance compared to any of the individual classifiers.[68] In order to improve the efficiency of the diagnosis procedure, this step utilizes several ensemble approaches including Bagging, Random Subspace, and Rotation Forest:

- Bagging, defined as bootstrap aggregation, is an ensemble learning method that reduces variance in a noisy set of data. Bagging chooses a random sample of data from a training instance with partial substitution, which means that single data points could be selected multiple times.
- Rotation Forest is a technique for creating classifier ensembles utilizing various feature sets. To generate data for training for a classification algorithm, the set of features is arbitrarily divided into K subsamples (K is an algorithm parameter), and principal component analysis (PCA) is performed on every subset.
- Random subspace approach is close to Bagging; however, the features are arbitrarily sampled for each classifier, which means that different feature subsets are utilized to train the base classifier.

Experiment installation and evaluation

Experiment installation. The CNNs constructed in this work have some hyper-parameters that are adjusted. Among these hyper-parameters is the epochs' amount which is tweaked to 50. Furthermore, the mini-batch size is modified to 5, and the learning rate is altered to 0.0003. Finally, the validation frequency is set to 80 and 31 for the MSID and MSLD datasets, respectively. To learn the CNNs, the stochastic gradient descent with momentum optimization strategy is being used. The 5-fold cross-validation is employed to access the performance of MonDiaL-CAD CAD. The base classifier for the ensemble learning approach is the linear SVM. The number of learners for Bagging and Rotation Forest is 10. Besides, the number of ensembles for Random Subspace is 50 and 20 for the MSID and MSLD datasets, respectively.

Evaluation indicators. To assess the efficacy of the proposed MonDiaL-CAD, four calculations are performed: True Negative (TN), False Negative (FN), True Positive (TP), and False Positive (FP). The above metrics describe examples of numbers that are either correctly or wrongly identified as monkeypox or negatives. The measures retrieved are employed to calculate various metrics including the sensitivity, precision, accuracy, F1 measure, specificity, as well as the Mathew correlation coefficient (MCC). Also, receiving operating characteristics curve (ROC) and the area under ROC (AUC) is employed. The evaluation metrics are described by the following equation:

$$Accuracy = \frac{TP + TN}{TN + FP + FN + TP} \quad (3)$$

$$Sensitivity = \frac{TP}{TP + FN} \quad (4)$$

$$Precision = \frac{TP}{TP + FP} \quad (5)$$

$$MCC = \frac{TP \times TN - FP \times FN}{\sqrt{(TP + FP)(TP + FN)(TN + FP)(TN + FN)}} \quad (6)$$

$$F1 - Score = \frac{2 \times TP}{(2 \times TP) + FP + FN} \quad (7)$$

$$Specificity = \frac{TN}{TN + FP} \quad (8)$$

Results

This section will be illustrating the results of the proposed MonDiaL-CAD. First, it will provide the accuracy of the SVM classifier used to score the deep features obtained from the eight CNNs employed in this work. Next, it will show the diagnostic accuracy attained by the fused deep feature sets generated with DWT and explored via the forward search strategy of MonDiaL-CAD. Afterward, it will deliver the results achieved after the presented entropy-based feature selection. Finally, it will demonstrate the performance of the ensemble classification procedure.

Deep feature scoring results

The classification accuracies of the SVM classifier trained individually with deep features acquired from every CNN are shown

Table 3. The classification accuracies (%) of the SVM classifier trained individually with deep features acquired from every CNN.

	MSID dataset	MSLD dataset
ResNet-18	94.1	94.3
ResNet-50	94.3	93.4
ResNet-101	94.8	95.2
Inception	94.1	92.1
MobileNet	92.2	93.0
Shuffle	93.6	93.0
Xception	94.5	96.1
DarkNet-53	93.6	93.4

in Table 3. The table shows that the highest accuracy of 94.8% and 96.1% are obtained using ResNet-101 and Xception for the MSID and MSLD datasets, respectively. On the other hand, the least performance is attained with MobileNet for the MSID dataset with an accuracy of 92.2%, while an accuracy of 92.1% is reached with Inception for the MSLD dataset. These classification accuracies shown in Table 3 are used to rank deep features and generate fused deep feature sets which are then employed to examine the best possible combination of deep features. Table 4 displays the fused deep feature sets produced after the ranking procedure.

Fused deep feature set exploration results

The classification accuracies attained using the SVM classifier during the exploration procedure for the best possible fused deep feature sets are demonstrated in Figure 4(a) and (b) for the MSID and MSLD datasets, respectively. It can be noted from Figure 4(a) that for the MSID dataset, the accuracy increases from Feature Set 1_MSID to Feature Set 3_MSID and then decreases afterward. This indicates that Feature Set 3_MSID consisting of the combined spatial-time-frequency features of Xception + ResNet-101 + ResNet-50 CNNs achieved the highest accuracy of 96.4% and is adequate to accomplish a diagnosis. There is no need to add deep features of more CNNs. Likewise, as noticed in Figure 4(b), there is a significant improvement in the classification accuracy until Feature Set 3_MSLD, and then no enhancement is noticed after that. These results prove that Feature Set 3_MSLD involving Xception + ResNet-101 + ResNet-18 CNNs trained with MSLD data is sufficient to accomplish the diagnosis (accuracy = 97.8%) adding extra deep feature from other CNNs is not required and does not increase performance

Table 4. Deep feature sets generated after the ranking procedure.

Deep feature set name	CNNs involved
MSID Dataset	
Feature Set 1_MSID	ResNet-101
Feature Set 2_MSID	Xception + ResNet-101
Feature Set 3_MSID	Xception + ResNet-101 + ResNet-50
Feature Set 4_MSID	Xception + ResNet-101 + ResNet-50 + ResNet-18
Feature Set 5_MSID	Xception + ResNet101 + ResNet-50 + Inception
Feature Set 6_MSID	Xception + ResNet101 + ResNet-50 + Shuffle
Feature Set 7_MSID	Xception + ResNet101 + ResNet-50 + DarkNet-53
Feature Set 8_MSID	Xception + ResNet101 + ResNet-50 + MobileNet
MSLD Dataset	
Feature Set 1_MSLD	Xception
Feature Set 2_MSLD	Xception + ResNet101
Feature Set 3_MSLD	Xception + ResNet101 + ResNet-18
Feature Set 4_MSLD	Xception + ResNet101 + ResNet-18 + ResNet-50
Feature Set 5_MSLD	Xception + ResNet101 + ResNet-18 + DarkNet-53
Feature Set 6_MSLD	Xception + ResNet101 + ResNet-18 + Shuffle
Feature Set 7_MSLD	Xception + ResNet101 + ResNet-18 + MobileNet
Feature Set 8_MSLD	Xception + ResNet101 + ResNet-18 + Inception

Deep feature selection results

This section describes the classification accuracies achieved after the entropy-based feature selection method. An ablation analysis is accomplished to determine the influence of differing the number of features on the performance of diagnosis. The outcome of the ablation study is displayed in Figure 5(a) and (b) for the MSID and MSLD datasets,

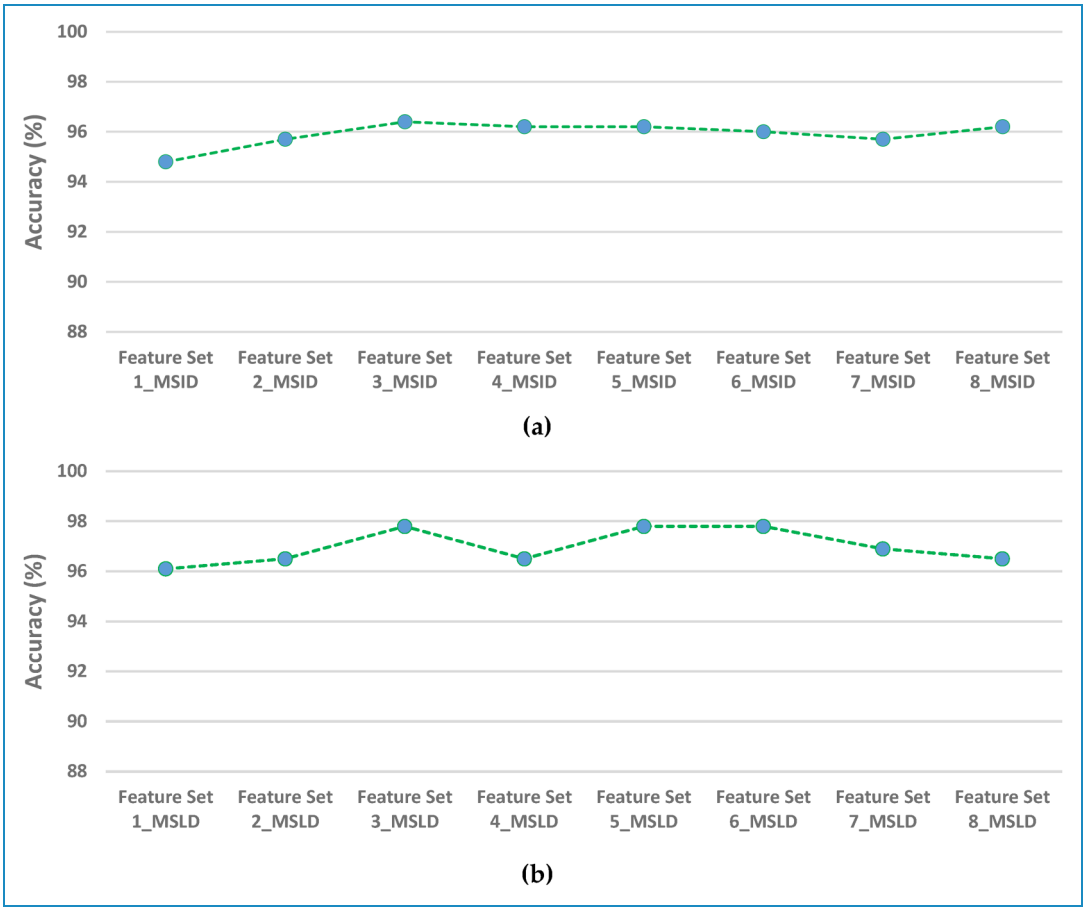

Figure 4. The classification accuracies attained using the SVM classifier during the exploration procedure for the best possible fused deep feature sets for (a) the MSID dataset and (b) the MSLD dataset.

respectively. Figure 5(a) demonstrates that for the MSID dataset, the maximum accuracy of 96.7% is attained with 600 and 700 merged deep features, and then the performance decays. This indicates that feature selection has improved the classification accuracy and lowered the number of features used in the diagnosis step. In contrast, the peak accuracy of 97.8% is achieved with 500 fused deep features as demonstrated in Figure 5(b). These findings displayed within Figure 5(b) show that the same accuracy is attained after feature selection; however, the amount of features employed is less which correspondingly decreases the complexity of the classification performance.

The confusion matrices are plotted and shown in Figure 6(a) and (b) for the MSID and MSLD datasets, respectively. It can be noted from Figure 6(a) that the sensitivity also described as the true positive rate (TPR) is equal to 94.6% and the specificity is equal to 98.7% for the MSID dataset, whereas for the MSLD dataset, the sensitivity and specificity correspond to 98.0% and 97.6% as shown in Figure 6(b). Furthermore, the ROC curves are displayed in Figure 7(a) and (b) for the MSID and MSLD datasets, correspondingly. These ROC curves indicate that the AUC for the MSID and MSLD datasets are equal to 0.99 and 0.99.

Ensemble learning results

This section illustrates the results after building the ensemble classifiers. The results of ensemble learning are demonstrated in Table 5. For the MSID dataset, both Bagging and Random Subspace have achieved the same accuracy of 0.971 where the sensitivity (0.957, 0.953), specificity (0.983, 0.987), precision (0.982, 0.985), F1-measure (0.969, 0.969), and MCC (0.941, 0.941) are accomplished for the Bagging and Random Subspace ensembles, respectively, whereas for Rotation Forest the accuracy, sensitivity, specificity, precision, F1-measure, and MCC are 0.967, 0.957, 0.977, 0.974, 0.966, and 0.934. In contrast, for the MSLD dataset, both Rotation Forest and Random Subspace have the exact accuracy and MCC of 0.982 and 0.965, while the sensitivity (0.980, 0.990), specificity (0.984, 0.976), precision (0.980, 0.971), and F1-measure (0.980, 0.981) are reached for Rotation Forest and Random Subspace, respectively. For Bagging a higher

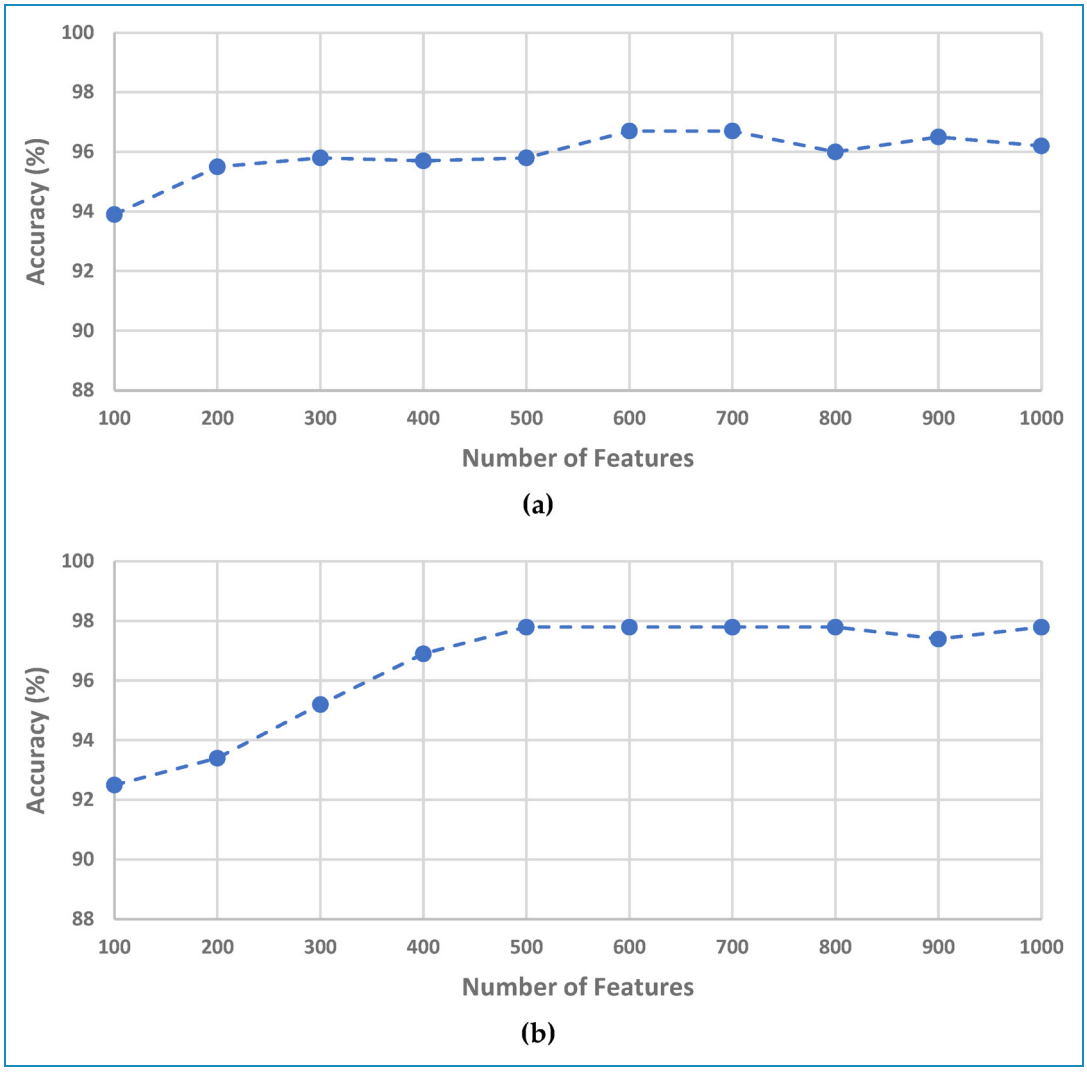

Figure 5. The classification accuracies (%) attained via the SVM classifier versus the number of deep features for (a) the MSID dataset and (b) the MSLD dataset.

accuracy of 0.987 is achieved. Moreover, the sensitivity, specificity, precision, F1-measure, and MCC values are equal to 0.990, 0.984, 0.981, 0.985, and 0.973 for Bagging.

Discussion

This work presents a CAD termed MonDiaL-CAD for the automatic diagnosis of monkeypox disease. MonDiaL-CAD initially acquires deep features from eight CNNs including ResNet-18, ResNet-50, ResNet-101, Shuffle, MobileNet, Inception, Xception, and DarkNet-53. It then employs deep features obtained from every CNN separately to train an SVM classifier. Next, the classification accuracy of this SVM classifier is used to rank these deep features. Afterward, these scores are used to generate several integrated deep feature sets using a forward search approach which guides the exploration for the best feasible blend of deep features instead of utilizing all deep features collected from all CNNs. In this step, DWT is employed to fuse each possible combination of deep features which reduces the size of features and results in the spatial-time-frequency presentation of features rather than only spatial. The selected fused deep feature set which achieved the highest performance then undergoes a feature selection procedure to further lessen the size of the combined features. Finally, the selected features are used to feed three ensemble classifiers to boost the performance.

The highest performance achieved with each stage of MonDiaL-CAD and the equivalent number of features used to train the classification model are assessed and displayed in Figure 8. Figure 8(a) shows that the classification accuracy is enhanced after fusing deep features of Xception + ResNet-101 + ResNet-50 for the MSID dataset and Xception + ResNet-101 + ResNet-18 for the MSLD dataset reaching an accuracy of 0.964 and 0.978. The results indicate that there is no need for using the deep features of other CNNs. This enhancement is also accompanied by a decrease in the

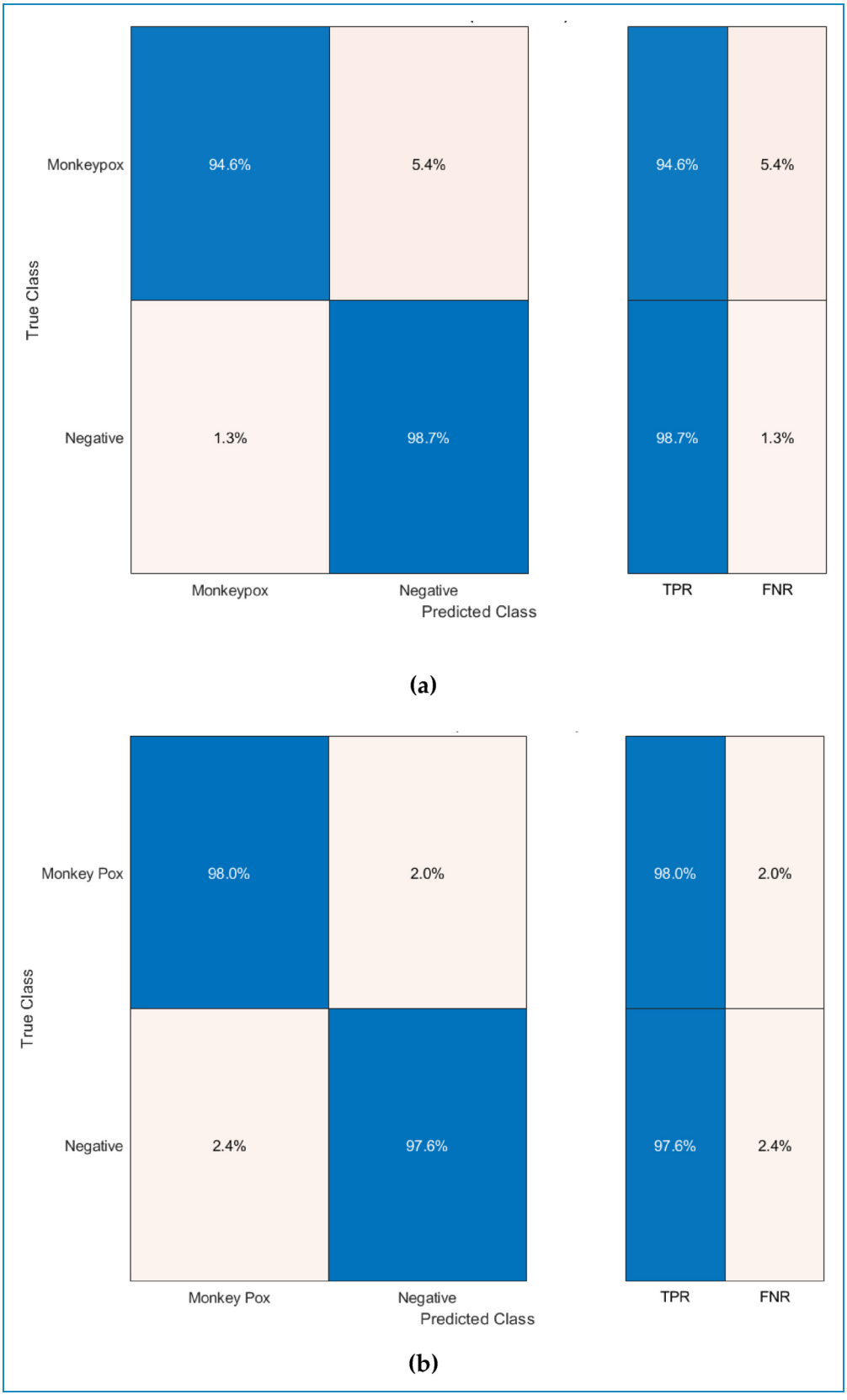

Figure 6. The confusion matrix achieved with the SVM classifier that was trained with the deep features selected. (a) the MSID dataset and (b) the MSLD dataset.

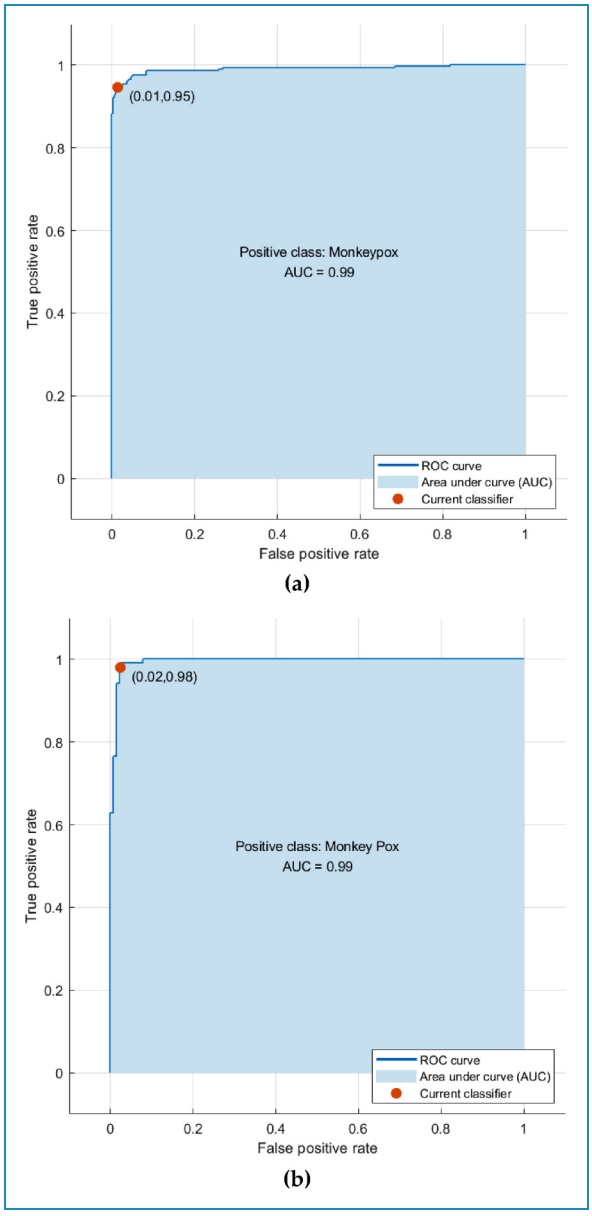

Figure 7. The ROC curve accomplished utilizing the SVM classifier trained with the selected deep features for (a) the MSID dataset and (b) the MSLD dataset.

number of features used to build the classification model from 2048 to 1536 and 1152 for the MSID and MSLD datasets as shown in Figure 8(b). Furthermore, this enhancement in accuracy verifies that employing the spatial-time-frequency features obtained with DWT in this step is superior to using spatial deep features only. Furthermore, the classification accuracy has further improved after utilizing the entropy-based feature selection for the MSID dataset (0.967), while it is the same for the MSLD dataset; however, the number of features is further reduced to 600 and 500 for the MSID and MSLD datasets, correspondingly. In addition, a further increase in the classification accuracy is achieved using ensemble classifiers, reaching 0.971 and 0.987 with Bagging for the MSID and MSLD datasets, correspondingly.

Comparisons

There are at present few articles that proposed CADs for monkeypox diagnosis. As a result, a broad comparison of our research results with previous research is narrow; however, a better-level evaluation of the presented performance measures remains viable. Table 6 shows a comparative study between MonDiaL-CAD and other previous CADs that performed binary classification using the same datasets. The results in Table 6 indicate that MonDiaL-CAD has a competing capability compared to other previous CAD. This is obvious as MonDiaL-CAD attained higher accuracy than most previous CADs. This is because they employed individual CNNs like,[3,36,42,45,52] did not perform feature selection,[12,42,45,52] or did not employ ensemble learning.[3,30,36,42,45,52] However, MonDiaL-CAD uses deep features from three CNNs. It also employs DWT to fuse features and reduce their dimension. Furthermore, it utilizes an entropy-based feature selection to further lower the size of features. Finally, MonDiaL-CAD adapts ensemble learning to boost performance. It is worth mentioning that the MSLD dataset has two editions: the original version and the augmented edition. The authors of reference[44] used the augmented edition of the dataset which contains versions of augmented images in both training and testing sets which led to this very high accuracy with only features of ResNet-18. In other words, the authors trained their model with augmented images that has close augmented replicas in the testing data which definitely lead to a very high-performance results. However, in the proposed model, the original edition of the MDSL dataset was utilized, and the images of the training set were only augmented to ensure that no replicas of the training images are included in the testing set of images.

On the other hand, the study[3] employed an optimization technique based on the AL-Biruni Earth radius stochastic fractal search (BERSFS). Although BERSFS improved the detection accuracy of the customized CNN, it has a very high computational cost which increases the complexity of the classification/detection process. Furthermore, the study[3] differentiated between monkeypox and chickenpox, measles, and healthy cases, whereas the proposed model distinguished between monkeypox and non-monkeypox cases.

Limitations of MonDiaL-CAD and future improvements

Numerous limitations have been encountered during the occurrence of the monkeypox illness that were outside of the scope of this study at the moment. The author highlights the following as research flaws that can be solved and improved in future work:

Table 5. The performance measures attained by ensemble classifiers for the MSID and MSLD datasets, respectively.

Ensemble	Accuracy	Sensitivity	Specificity	Precision	F1-measure	MCC
MSID Dataset						
Bagging	0.971	0.957	0.983	0.982	0.969	0.941
Rotation Forest	0.967	0.957	0.977	0.974	0.966	0.934
Random Subspace	0.971	0.953	0.987	0.985	0.969	0.941
MSLD Dataset						
Bagging	0.987	0.990	0.984	0.981	0.985	0.973
Rotation Forest	0.982	0.980	0.984	0.980	0.980	0.965
Random Subspace	0.982	0.990	0.976	0.971	0.981	0.965

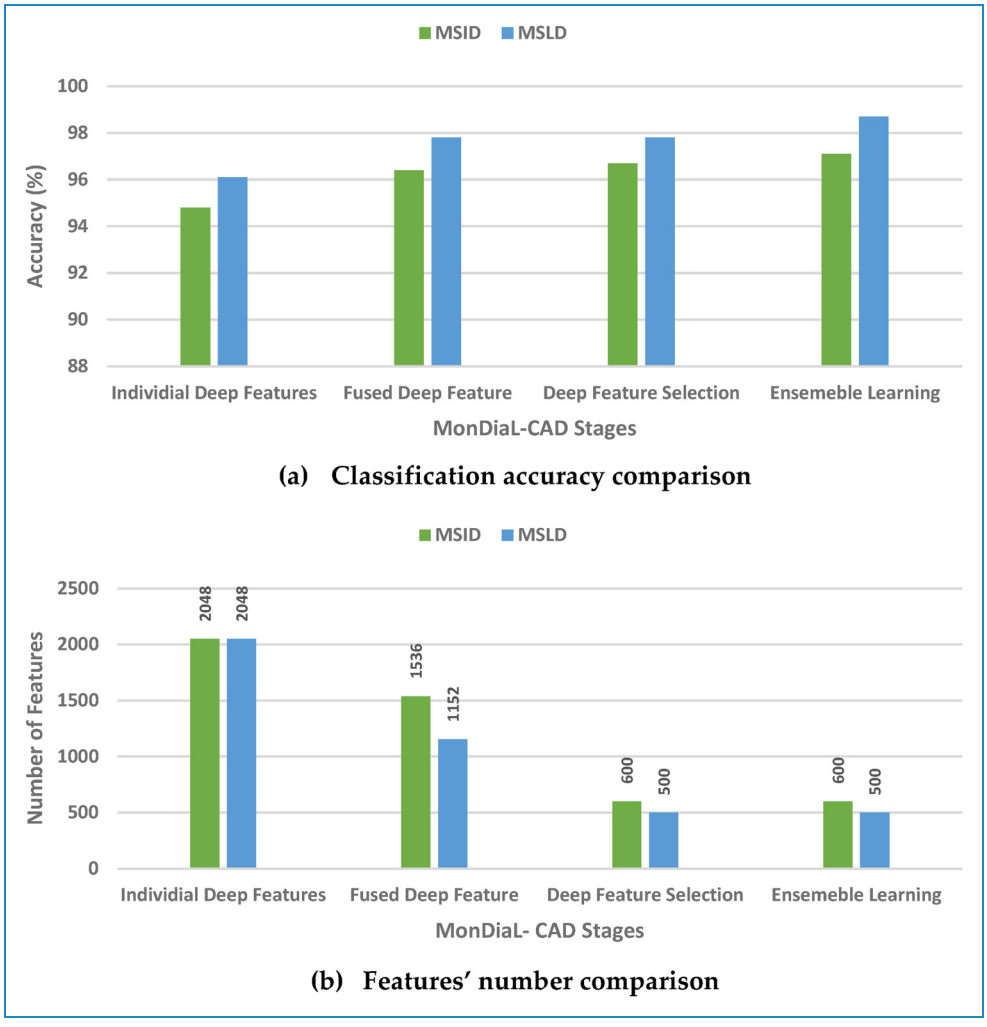

Figure 8. MonDiaL-CAD stages performance comparison; (a) the highest accuracy achieved with each stage of MonDiaL-CAD and (b) the corresponding features' amount employed to feed the classification model.

Table 6. Comparison study between the performance of MonDiaL-CAD and other earlier CAD that performed classification using the MSID and MSLD datasets.

Study	Dataset	Methods	Accuracy
[42]	MSLD	MobileNet	91.11%
[44]	MSLD	ResNet-18	99.81%
[45]	MSLD	MiniGoogLeNet	97.08%
[30]	MSLD	Inception + Xception + DenseNet-169 + Beta function-based normalization method	93.39%
[31]	MSLD	EfficientB0 + DenseNet	94.57%
[3]	MSID	customized CNN + BERSFS	98.83%
[36]	MSID	GoogLeNet + BER + SC + PS + MLP	93.8%
[12]	MSID	HHO + VGG-19 + RF + SVM + Majority voting	97.67%
[52]	Customized Dataset + MSLD	MobileNet	96.8%
MonDiaL-CAD	MSID	(Xception + ResNet-101 + ResNet-50) + DWT + FS + Bagging	97.1%
	MSLD	(Xception + ResNet-101 + ResNet-18) + DWT + FS + Bagging	98.7%

- Availability of data is a massive obstacle since there is no large dataset accessible. The above makes data authentication schemes like interpretation and utilization difficult. This factor limits the availability of benchmark literature. The insufficiency of relevant literature makes it difficult to conduct a fair assessment to evaluate the performance of the MonDiaL-CAD.
- One of the chief aspects of this restricted accessibility of data is the violation of privacy. Because monkeypox commonly affects the whole body, it is regularly difficult to find and use photographs of diseased faces images, especially for kids. Nevertheless, a variety of public repositories are continuously collecting new images to increase the volume of information available. As a result, data scarcity concerns may be alleviated in the coming days, but such datasets may be used in future studies to investigate the actual effectiveness of the proposed CAD.
- Furthermore, because monkeypox is uncommon, the illness is understudied. As a result, healthcare professionals that are experts in such condition is limited. Subsequently, it can result in the ailment not being properly diagnosed, resulting in illness propagation and ultimate epidemic.
- The datasets utilized were mostly gathered from public sources instead of medical centers or hospitals. Moreover, such datasets comprise a relatively small number of images. Also, it currently contains a small number of distinct patients. As a result, the MonDiaL-CAD's generalizability is limited. Future work will address this issue by adding more samples and more patient images from health facilities and hospitals to improve generalizability.
- This study did not consider other clinical features and patient data such as age, gender, and physical condition. Upcoming work will address this concern by adding this during the construction of the future CAD.
- The study did not involve an optimization technique for fine-tuning the CNNs' hyper-parameters, and upcoming work will address this issue.
- Future work will consider using optimization techniques such as AL-Biruni Earth radius stochastic fractal Search (BERSFS) to improve performance.

Conclusion

This work proposed a CAD called MonDiaL-CAD for diagnosing monkeypox disease automatically and accurately. In order to construct and validate the performance of MonDiaL-CAD, two datasets that were collected from online sources were utilized known as the MSID and MSLD datasets. MonDiaL-CAD CAD begins by obtaining deep features from eight CNNs. The deep features extracted from each CNN are then employed to learn an SVM classifier. Following that, the SVM classifiers' classification accuracy is utilized to sort these deep features. Next, the above

scores are applied to create multiple unified deep feature sets using a forward search algorithm, which instructs the search for the best available composite of deep features rather than incorporating the entire deep feature sets obtained from all CNNs. During the fusion phase, DWT is used to merge every possible combination of deep features, lowering feature size and resulting in a spatial-time-frequency demonstration of features instead of solely spatial information. The fused deep feature set with the best performance is then subjected to a feature selection method to lower the combined feature dimensions even further. Eventually, the chosen features are fed to three ensemble classifiers to improve performance. The result verified that combining deep features of only three CNNs achieved the highest classification accuracy, thus there is no necessity to add more deep features from other CNNs which increases the complexity and duration of training of the classification model. Furthermore, merging deep features with DWT has revealed the time-frequency representations of the spatial deep feature. Training the classification model with these spatial-time-frequency representations has enhanced performance and lowered the feature space dimensionality thus lowering its complexity. The entropy-based feature selection when applied to the best combination of deep features has successfully lowered the dimension of features achieving at least the same classification accuracy. Lastly, the three ensemble classifiers have a further enhancement in the classification accuracy. Furthermore, the results of MonDiaL-CAD are compared to prior CADs to show the effectiveness of the proposed procedure. The comparative study revealed that the proposed method outperformed most of the existing CADs. Because the proposed CAD achieved promising results utilizing deep learning algorithms such as CNNs and TL, it will strongly urge researchers and clinicians to use CNNs and TL methodologies to create and implement CNN-based monkeypox diagnosis in clinical settings.

Acknowledgments: Not applicable

Contributorship: Omneya Attallah is the only contributor to this work.

Data availability statement: MSID dataset is accessible through the following link: https://www.kaggle.com/datasets/dipuiucse/monkeypoxskinimagedataset.
MSLD dataset is accessible through the following link: https://www.kaggle.com/datasets/nafin59/monkeypox-skin-lesion-dataset.

Declaration of conflicting interests: The author(s) declared no potential conflicts of interest with respect to the research, authorship, and/or publication of this article.

Funding: The author(s) received no financial support for the research, authorship, and/or publication of this article.

Guarantor: The author Omneya Attallah will be the guarantor of this manuscript.

Institutional review board statement: Not applicable.

Informed consent statement: Not applicable.

ORCID iD: Omneya Attallah https://orcid.org/0000-0002-2657-2264

Supplemental material: Supplemental material for this article is available online.

References

1. McCollum AM and Damon IK. Human monkeypox. *Clin Infect Dis* 2014; 58: 260–267.
2. Ferdous J, Barek MA, Hossen MS, et al. A review on monkeypox virus outbreak: new challenge for world. *Health Sci Rep* 2023; 6: e1007.
3. Khafaga DS, Ibrahim A, El-Kenawy ESM, et al. An Al-Biruni Earth Radius Optimization-based deep convolutional neural network for classifying monkeypox disease. *Diagnostics* 2022; 12: 2892.
4. Dada EG, Oyewola DO, Joseph SB, et al. Ensemble machine learning for monkeypox transmission time series forecasting. *Appl Sci* 2022; 12: 12128.
5. Zumla A, Valdoleiros SR, Haider N, et al. Monkeypox outbreaks outside endemic regions: scientific and social priorities. *Lancet Infect Dis* 2022; 22: 929–931.
6. Sitaula C and Shahi TB. Monkeypox virus detection using pre-trained deep learning-based approaches. *J Med Syst* 2022; 46: 78.
7. Attallah O and Samir A. A wavelet-based deep learning pipeline for efficient COVID-19 diagnosis via CT slices. *Appl Soft Comput* 2022; 128: 109401.
8. Attallah O. RADIC: a tool for diagnosing COVID-19 from chest CT and X-ray scans using deep learning and quad-radiomics. *Chemom Intell Lab Syst* 2023; 233: 104750.
9. Attallah O. Deep learning-based CAD system for COVID-19 diagnosis via spectral-temporal images. In: 2022 the 12th international conference on information communication and management, London, UK, 2022, pp.25–33.
10. Fang Y, Zhang H, Xie J, et al. Sensitivity of chest CT for COVID-19: comparison to RT-PCR. *Radiology* 2020; 296: E115–E117.
11. Attallah O. A computer-aided diagnostic framework for coronavirus diagnosis using texture-based radiomics images. *DIGITAL HEALTH* 2022; 8: 20552076221092544.
12. Almutairi SA. DL-MDF-OH2: optimized deep learning-based monkeypox diagnostic framework using the metaheuristic Harris Hawks Optimizer Algorithm. *Electronics (Basel)* 2022; 11: 4077.
13. Ghanem NM, Attallah O, Anwar F, et al. AUTO-BREAST: a fully automated pipeline for breast cancer diagnosis using AI technology. In: *Artificial intelligence in cancer diagnosis and prognosis, volume 2: breast and bladder cancer*. Bristol, UK: IOP Publishing, 2022, pp.6–1–6–24.

14. Attallah O, Anwar F, Ghanem NM, et al. Histo-CADx: duo cascaded fusion stages for breast cancer diagnosis from histopathological images. *PeerJ Computer Science* 2021; 7: e493.
15. Anwar F, Attallah O, Ghanem N, et al. Automatic breast cancer classification from histopathological images. In: 2019 international conference on advances in the emerging computing technologies (AECT), 2020, pp.1–6. IEEE.
16. Attallah O. MB-AI-His: histopathological diagnosis of pediatric medulloblastoma and its subtypes via AI. *Diagnostics* 2021; 11: 359–384.
17. Attallah O and Zaghlool S. AI-based pipeline for classifying pediatric medulloblastoma using histopathological and textural images. *Life* 2022; 12: 232.
18. Attallah O. CoMB-deep: composite deep learning-based pipeline for classifying childhood medulloblastoma and its classes. *Front Neuroinform* 2021; 15: 663592.
19. Attallah O. An effective mental stress state detection and evaluation system using minimum number of frontal brain electrodes. *Diagnostics* 2020; 10: 292–327.
20. Attallah O and Sharkas M. GASTRO-CADx: a three stages framework for diagnosing gastrointestinal diseases. *PeerJ Comput Sci* 2021; 7: e423.
21. Attallah O. GabROP: gabor wavelets-based CAD for retinopathy of prematurity diagnosis via convolutional neural networks. *Diagnostics* 2023; 13: 171.
22. Attallah O. DIAROP: automated deep learning-based diagnostic tool for retinopathy of prematurity. *Diagnostics* 2021; 11: 2034.
23. Attallah O, Ibrahim RA and Zakzouk NE. CAD System for inter-turn fault diagnosis of offshore wind turbines via multi-CNNs & feature selection. *Renewable Energy* 2023; 203: 870–880.
24. Attallah O, Ibrahim RA and Zakzouk NE. Fault diagnosis for induction generator-based wind turbine using ensemble deep learning techniques. *Energy Rep* 2022; 8: 12787–12798.
25. Attallah O and Morsi I. An electronic nose for identifying multiple combustible/harmful gases and their concentration levels via artificial intelligence. *Measurement (Mahwah N J)* 2022; 199: 111458.
26. Attallah O. Tomato leaf disease classification via compact convolutional neural networks with transfer learning and feature selection. *Horticulturae* 2023; 9: 149.
27. Almufareh MF, Tehsin S, Humayun M, et al. A transfer learning approach for clinical detection support of monkeypox skin lesions. *Diagnostics* 2023; 13: 1503.
28. Naveen CV, Abhiram G, Aneesh V, et al. Monkeypox detection using transfer learning, ResNet50, Alex Net, ResNet18 & custom CNN model. *Asian J Adv Res Rep* 2023; 17: 7–13.
29. Anwar SM, Majid M, Qayyum A, et al. Medical image analysis using convolutional neural networks: a review. *J Med Syst* 2018; 42: 1–13.
30. Pramanik R, Banerjee B, Efimenko G, et al. Monkeypox detection from skin lesion images using an amalgamation of CNN models aided with Beta function-based normalization scheme. *PLoS One* 2023; 18: e0281815.
31. Liu W. Implementation of detection of skin lesions in monkeypox based on a deep learning model: using an improved bilinear pooling model. In: Second International Conference on Biological Engineering and Medical Science (ICBioMed 2022), 2023, pp.212–219, SPIE.
32. Zhou T, Lu H, Yang Z, et al. The ensemble deep learning model for novel COVID-19 on CT images. *Appl Soft Comput* 2021; 98: 106885.
33. Chakraborty J and Nandy A. Discrete wavelet transform based data representation in deep neural network for gait abnormality detection. *Biomed Signal Process Control* 2020; 62: 102076.
34. Ladnyj ID, Ziegler P and Kima E. A human infection caused by monkeypox virus in Basankusu Territory, Democratic Republic of the Congo. *Bull W H O* 1972; 46: 593.
35. Bragazzi NL, Kong JD, Mahroum N, et al. Epidemiological trends and clinical features of the ongoing monkeypox epidemic: a preliminary pooled data analysis and literature review. *J Med Virol* 2023; 95: e27931.
36. Abdelhamid AA, El-Kenawy ESM, Khodadadi N, et al. Classification of monkeypox images based on transfer learning and the Al-Biruni Earth Radius Optimization algorithm. *Mathematics* 2022; 10: 3614.
37. Chadaga K, Prabhu S, Sampathila N, et al. Application of artificial intelligence techniques for monkeypox: a systematic review. *Diagnostics* 2023; 13: 824.
38. Niu S, Liu Y, Wang J, et al. A decade survey of transfer learning (2010–2020). *IEEE Trans Artif Intell* 2020; 1: 151–166.
39. Weiss K, Khoshgoftaar TM and Wang D. A survey of transfer learning. *J Big Data* 2016; 3: 1–40.
40. Ahsan MM, Uddin MR and Luna SA. Monkeypox image data collection. *arXiv preprint arXiv:2206.01774*. 2022.
41. Ahsan MM, Uddin MR, Farjana M, et al. Image data collection and implementation of deep learning-based model in detecting Monkeypox disease using modified VGG16. *arXiv preprint arXiv:2206.01862*. 2022.
42. Sahin VH, Oztel I and Yolcu Oztel G. Human monkeypox classification from skin lesion images with deep pre-trained network using mobile application. *J Med Syst* 2022; 46: 79.
43. Ali SN, Ahmed M, Paul J, et al. Monkeypox skin lesion detection using deep learning models: a feasibility study. *arXiv preprint arXiv:2207.03342*. 2022.
44. Islam A and Shin SY. A blockchain-based privacy sensitive data acquisition scheme during pandemic through the facilitation of federated learning. In: 2022 13th international conference on information and communication technology convergence (ICTC), 2022, pp.83–87, IEEE.
45. Alcalá-Rmz V, Villagrana-Bañuelos KE, Celaya-Padilla JM, et al. Convolutional neural network for monkeypox detection. In: Proceedings of the international conference on ubiquitous computing & ambient intelligence (UCAmI 2022), 2022, pp.89–100, Springer.
46. Celaya-Padilla JM, Galván-Tejada JI, Gamboa-Rosales H, et al. Convolutional neural network for monkeypox detection. In: Proceedings of the international conference on ubiquitous computing & ambient intelligence (UCAmI 2022), Vol. 594, 2022, p.89, Springer Nature.
47. Bala D. Monkeypox Skin Images Dataset (MSID). 2022.
48. Irmak MC, Aydin T and Yağanoğlu M. Monkeypox skin lesion detection with MobileNetV2 and VGGNet models. In: 2022 medical technologies congress (TIPTEKNO), 2022, pp.1–4, IEEE.
49. Bala D, Hossain MS, Hossain MA, et al. Monkeynet: a robust deep convolutional neural network for monkeypox disease detection and classification. *Neural Netw* 2023; 161: 757–775.

50. Uzun Ozsahin D, Mustapha MT, Uzun B, et al. Computer-aided detection and classification of monkeypox and chickenpox lesion in human subjects using deep learning framework. *Diagnostics* 2023; 13: 292.
51. Ahsan MM, Uddin MR, Ali MS, et al. Deep transfer learning approaches for monkeypox disease diagnosis. *Expert Syst Appl* 2023; 216: 119483.
52. Altun M, Gürüler H, Özkaraca O, et al. Monkeypox detection using CNN with transfer learning. *Sensors* 2023; 23: 1783.
53. Manna A, Kundu R, Kaplun D, et al. A fuzzy rank-based ensemble of CNN models for classification of cervical cytology. *Sci Rep* 2021; 11: 1–18.
54. Attallah O. A deep learning-based diagnostic tool for identifying various diseases via facial images. *Digital Health* 2022; 8: 20552076221124430.
55. Ali H, Sharif M, Yasmin M, et al. A survey of feature extraction and fusion of deep learning for detection of abnormalities in video endoscopy of gastrointestinal-tract. *Artif Intell Rev* 2019; 53: 1–73.
56. Attallah O. ECG-BiCoNet: an ECG-based pipeline for COVID-19 diagnosis using Bi-layers of deep features integration. *Comput Biol Med* 2022; 142: 105210.
57. ÇELİK M and Özkan İ. Detection of monkeypox among different pox diseases with different pre-trained deep learning models. *J Inst Sci Technol* 2023; 13: 10–21.
58. ÖRENÇ S, Emrullah A and ÖZERDEM MS. Utilizing the ensemble of deep learning approaches to identify monkeypox disease. *Dicle Üniv Mühendis Fak Mühendis Derg* 2022; 13: 685–691.
59. Miko\lajczyk A and Grochowski M. Data augmentation for improving deep learning in image classification problem. In: 2018 international interdisciplinary PhD workshop (IIPhDW), 2018, pp.117–122, IEEE.
60. Attallah O. An intelligent ECG-based tool for diagnosing COVID-19 via ensemble deep learning techniques. *Biosensors* 2022; 12: 299.
61. Burger W, Burge MJ, Burge MJ, et al. *Principles of digital image processing*. Vol. 111. London, UK: Springer, 2009.
62. Attallah O. Cervical cancer diagnosis based on multi-domain features using deep learning enhanced by handcrafted descriptors. *Appl Sci* 2023; 13: 1916.
63. Alhenawi E, Al-Sayyed R, Hudaib A, et al. Feature selection methods on gene expression microarray data for cancer classification: a systematic review. *Comput Biol Med* 2022; 140: 105051.
64. Chandrashekar G and Sahin F. A survey on feature selection methods. *Comput Electr Eng* 2014; 40: 16–28.
65. Attallah O, Karthikesalingam A, Holt PJE, et al. Using multiple classifiers for predicting the risk of endovascular aortic aneurysm repair re-intervention through hybrid feature selection. *Proc Inst Mech Eng H: J Eng Med* 2017; 231: 1048–1063.
66. Abe N and Kudo M. Entropy criterion for classifier-independent feature selection. In: Knowledge-based intelligent information and engineering systems: 9th international conference, KES 2005, Melbourne, Australia, September 14–16, 2005, Proceedings, Part IV 9, 2005, pp.689–695, Springer.
67. Wu Y. An information entropy embedding feature selection based on genetic algorithm. *Secur Commun Netw* 2022; 2022: 1–10.
68. Bramer M. Ensemble classification. In: *Principles of data mining. Undergraduate topics in computer science*. London, UK: Springer, 2013.